8th EnvImeko - IMEKO TC19 Symposium on Environmental Instrumentation and Measurements
October 29-30, 2019, Sfax, Tunisia

Design and Investigation on Flexible Inductive Power Tranmission Shields

Ghada Bouattour[1,2], Ayda Bouhamed[1], Ammar Al-Hamry[1], Rajarajan Ramalingame[1], Houda Ben Jmeaa Derbel[2], Olfa Kanoun[1]

[1]Chair for Measurement and Sensor Technology, Technische Universität Chemnitz, Chemnitz, Germany
[2]Department of Electrical Engineering, National Engineering School of Sfax, University of Sfax, Sfax, Tunisia

***Abstract*—Inductive power transmission coils are more and more used to charge devices wirelessly. In many applications, robustness, small size and flexibility of the used coils are required. For that, a design of flexible coil associated to a flexible ferrite shield becomes a necessity in order to achieve an efficient power transfer. In this paper, a new material composition for the ferrite shield have been proposed. It guarantees a better flexibility and performance using a simple fabrication process. Therefore, an optimization of the ferrite shield concentrations and thicknesses are performed. The influence of different prepared ferrite shield on the coil self-inductance and quality factor are investigated. Results shows that a concentration of ferrite of about 85 wt. % present the highest efficiency in case of high thickness with a self-inductance of 20.5 µH while in low concentration the measured coil self-inductance is around 17.5 µH.**

Keywords*—*Wireless Power Transmission, Inductive Power Transmission, Flexible Shield, Flexible Coil, Efficiency,

I. Introduction

Nowadays, various wireless charging systems are developed [1] such as capacitive charging [2], radio frequency energy harvesting [3], and Inductive Power Transmission (IPT) systems [4-6] to supply different applications including medical devices charging [7], electrical vehicles [8], costumer electronics [9] and robot charging [10]. Comparison between various systems shows that charging via inductive links offer better efficiency and resistance to harsh environment.

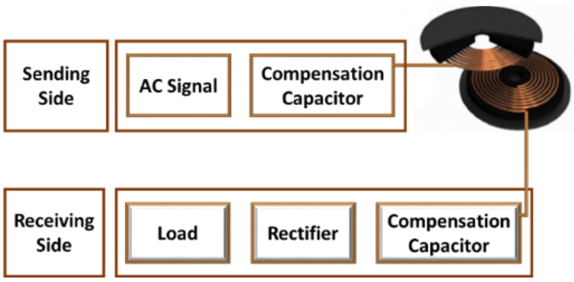

Fig. 1. General structure of an inductive power transmission systems.

Usually, the structure of IPT is composed by sending and receiving sides as illustrated in Fig. 1. In the sending side, an AC signal generator is exciting the sending coil (L_s) to generate magnetic field. The generated magnetic field induces voltage across the receiving coil (L_r) to charge the load.

Two kind of coils, air core coils and ferrite core coils can be used in IPT systems. The air core coil is formed by only several turns of copper wires. The ferrite core coils is composed by an air core coil associated to an additional ferrite shield. In [11], authors discuss the influence of metallic material in different ranges of frequencies for IPT systems. Results shows metallic material in low frequencies increases the system efficiency where the high frequency decrease the system losses due to eddy current behavior. For that, the air-core coils [4] are used in case of high frequency application, which requires high flexibility or/and small thickness of the coil. However, the additional ferrite shield has several advantages such as isolating the coil to other metallic objects of the system and increasing the coil self-inductance and system efficiency. However, the existing ferrite shields possess can be high rigidity making them easy to break in case of falls as shown in Fig.2 (a) or flexible with a short lifetime when they are bended as mentioned in Fig. 2 (b).

(a) (b)

Fig. 2. Broken commercial ferrit shileds (a) Solid shiled (b) Flexible shiled.

In addition, there are many other challenging aspects of ferrite shield layers was related to the IPT performance such as the dimensions, the thickness and the used material properties. In [12], a commercial ferrite shield with small thickness was presented. It was characterized by their proper reflection behavior, a reduction of the shield robustness and thickness. In [13], authors compare between different metallic materials such as copper and iron. Results shows that the iron increases the transmission efficiency where copper reduce it due to their high eddy current absorption behavior. Focusing on shield robustness, in [14], authors present a material composition based on soft magnetic composite which can tolerate a fall of 1 m. However, the developed layer still has a big thickness and a high rigidity, which reduce the integrity of the coil in flexible system. In [15], authors developed a 3D printed coil and a flexible ferrite material to increase the coil flexibility with small thickness. However, it presents a small ferrite concentration and the manufacturing proses is very complexity and costly.

In this paper, a simple and cost-effective preparation process of highly flexible ferrite shield layer was proposed. A study of the influence of different ferrite thickness with different concentrations on is presented.

II. THEORETICAL BEGROUND OF MUTUAL IMPEDANCE

The design of the coil depends on several parameters which define the coil. The real models of the sending and receiving coils are composing of inductor (L_S) connected to an equivalent resistance (R_{LS}) with a parallel parasitic capacitance () as presented in Fig.3.

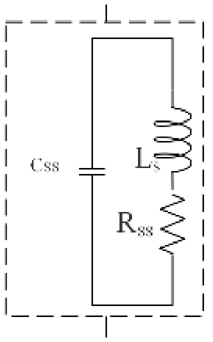

Fig. 3. Simplified electrical coils model.

The coil design influence in a good way on the system efficiency. Eq.1 presents the maximum reached efficiency of an IPT system which depends on the sending and receiving coils quality factors (Q_1, Q_2 respectively) and the coupling factor between the both coils. The quality factors of the sending and receiving coils are presented in Eq. 2 and Eq. 3, respectively. They depend on the working frequency and the both coils self-inductances and internal resistances, which can be illustrated by the quality factors of the sending and the receiving coils, respectively.

$$\eta = \frac{k^2 Q_1 Q_2}{\left(1+\sqrt{(1+k^2 Q_1 Q_2)}\right)^2} \quad (1)$$

$$Q_1 = \frac{\omega L_S}{R_{SS}} \quad (2)$$

$$Q_2 = \frac{\omega L_S}{R_{Sr}} \quad (3)$$

$$k = \frac{M}{\sqrt{L_1 L_2}} \quad (4)$$

M is the equivalent mutual inductance between the sending and receiving coil. It depends on several parameters such as number of turns and different coil parameters and geometries.

Fig.4 (a), shows an illustration of ferrite core sending coil with an air core receiving coil. Fig.4 (b) present the presented coil cross sections of the used system with their parameters.

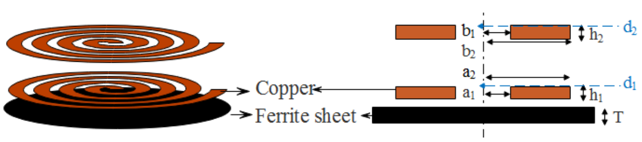

(a) (b)

Fig. 4. (a) Illustration of the coil (b) cross section

In [13], authors develop an analytical model of the mutual inductance in case of finite substrate thickness and with pure ferrite shield can be defined in Eq. 5 to Eq. 11.

$$Z_{i,j} = j\omega M_{i,j} + Z_{sub.i,j} \quad (5)$$

$$Z_{sub.i,j} = RZ_{sub.i,j} + jIZ_{sub.i,j} \quad (6)$$

$$M = M_{i,j} + \frac{IZ_{sub.i,j}}{\omega} \quad (7)$$

In fact, the equivalent mutual inductance as presented in Eq. 8 depends on two major parameters $M_{i,j}$ and $IZ_{sub.i,j}$ where $M_{i,j}$ the mutual inductance between two air coils is and $IZ_{sub.i,j}$ present the inductive reactance due to the presence of ferrite materiel under the coil. In fact, $IZ_{sub.i,j}$ is the imaginary part of the additional impedance ($Z_{sub.i,j}$) presented in Eq. 10. The total system impedance presented in Eq.6 present equivalent the mutual inductance and the losses due to the eddy current between the coil and the shield illustrated by the real part $Z_{sub.i,j}$. The air core coils mutual inductance is defined in Eq. 9 using elliptic integrals [4] where K(f) and E(f) are the first and the second kinds of the complete elliptic integrals, respectively.

$$M_{i,j} = \mu_0 \sqrt{ar}\frac{2}{f}\left[\left(1-\frac{f^2}{2}\right)K(f) - E(f)\right] \quad (8)$$

Where

$$f = \sqrt{\frac{4ar}{d^2+(a+r)^2}} \quad (9)$$

$$d = |d_b - d_a|$$

The additional impedance $Z_{sub.i,j}$ is presented in Eq.10 to Eq.16, which depends on used ferrite materials such as thickness and material properties.

$$Z_{i,j} = \frac{j\omega\pi\mu_0}{h_a h_b ln\left(\frac{a_2}{a_1}\right) ln\left(\frac{b_2}{b_1}\right)} \int_0^{\infty} C(u) e^{-ud} du \quad ()$$

Where

$$C(u) = S(ua_2, ua_1) S(uab_2, ub_1) Q(uh_a, uh_b)\, \gamma(T) \quad (11)$$

$$S(ux, uy) = \frac{J_0(ux) - J_0(uy)}{u} \quad (12)$$

$$Q(ux, uy) = \frac{2}{u^2}\left[\cosh\left(u\frac{x+y}{2}\right) - \cosh\left(u\frac{x-y}{2}\right)\right] \quad (13)$$

$$\gamma(T) = \emptyset(u)\frac{1-e^{-2\Psi T}}{1-\emptyset(u)^2 e^{-2\Psi T}} \quad (14)$$

$$\emptyset(u) = \frac{\mu_r - \frac{\Psi}{u}}{\mu_r + \frac{\Psi}{u}} \quad (15)$$

$$\Psi = \sqrt{u^2 + j\omega\mu_r\mu_0\sigma} \quad (16)$$

Equations shows that the mutual inductance depend on the ferrite shield substrate characteristics such as thickness, conductivity and permeability. In this case, the conductivity and the permeability of the ferrite shield vary due to their different concentration on the integrated shield. For that, an experimental investigation of different concentration and thickness has been proposed in this paper.

III. DESIGN OF INDUCTIVE POWER TRANSMISSION FERRITE SHIELD

To investigate the ferrite influence on the coil behavior, different ferrite concentrations has been studied. The ferrite powder (Fe) concentration is expressed in Eq. 17, which depends on the ferrite weight (m_f) and the polymer weight ($m_{Polymer}$). By increasing the ferrite concentrations, the obtained solution characteristics vary such as the material fluidity which limit the maximum investigated ferrites concentration to 85 wt. %.

$$C = \frac{m_f}{m_{Polymer} + m_f} . 100 \quad (17)$$

A fabrication of ferrite shields with different two thicknesses and variable concentration is presented. To increase more the thickness of the ferrite shield, multi-layers of shields are associated together with minimum of air between them.

(a) (b)

Fig. 5. Experimental setup (a) Proposed flexible shield (b) Thickness measurement.

A prototype of the obtained ferrite shield is presented in Fig.5 (a). For that, a thickness of shieling is measured to verify the final samples thickness (Fig.5 (b)) and to measure the error range and their influence on the final coil parameters.

$$A_T = \frac{\sum_{i=1}^{n} T_i}{n} \quad (18)$$

$$\mathrm{E} = \max(|T_i - A_T|_{i=1..n}) \quad (19)$$

Table I present a summary of the measured thickness in case of different samples (S1 to S10) concentrations, the average of thickness (A_T) presented in Eq.18 and the maximum thickness error between the designed samples (E) presented in Eq.19 where T_i the thickness of the sample number i.

TABLE I. MEASURED THICKNESS FOR DIFFERENT CONCENTRATIONS

Tested samples	**Ferrite shield parameters**		
	Concentration (wt. %)	***Thicknesses***	
		T1 (mm)	***T2 (mm)***
S0	0	-	
S1	33.33	0.26	0.41
S2	37.5	0.27	0.47
S3	41.17	0.31	0.39
S4	50	0.31	0.37
S5	57.14	0.21	0.37
S6	65	0.25	0.41
S7	70	0.26	0.42
S8	75	0.22	0.4
S9	80	0.23	0.5
S10	85	0.34	0.49
Average of thickness (A_T)		0.27	0.42
Maximum thickness error (E)		0.07	0.08

IV. EXPERIMENTAL SETUP AND RESULTS

A. Measurement procedure

To measure the coils parameters such as mutual inductance, self-inductance and quality factor, an Impedance Analyzer (IA) has been used. The used sending and receiving air core coils radius are 10 mm and 6 mm, respectively where their measured self-inductances are 21 µH and 17.1 µH, respectively. The used coils quality factor in case of no shields was equal to 18.16. During the investigation, the sending coil was place placed above the designed shields as shown in Fig.8.

The measurement of the coupling factor was done for a fixed frequency equal to 100 kHz in case of ideal alignment and minimum distance between sending and receiving coils. The measurement procedure was described in [13] and illustrated in Fig.6, starts by measuring the sending coil self-inductance L_{2open}, L_{2short} in case of open circuit and short-circuited receiving coil, respectively (Fig.6 (a) and (b)). Then, it is the required position a measurement of the receiving coil self-inductance L_{1open} when the sending coil is open circuited as presented in Fig.6 (c).

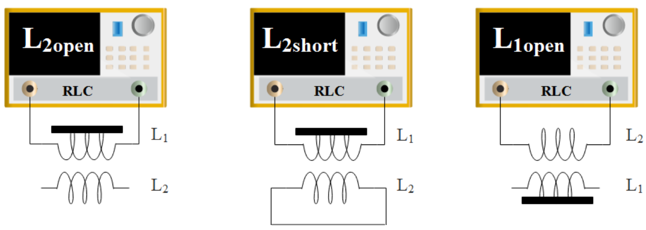

(a) (b) (c)

Fig. 6. Coupling factor measurement procedure (a) Measurement of L_{2open} (b) Measurement of L_{2short} (c) Measurement of L_{1open}

The experimental equivalent mutual inductance (M) and coupling factor (k) is then calculated as presented in Eq.20 and Eq.21.

$$\mathrm{M} = \sqrt{(L_{2open} - L_{2short})L_{1open}} \quad (20)$$

$$\mathrm{K} = \frac{\sqrt{L_{2open} - L_{2short}}}{\sqrt{L_{2open}}} \quad (21)$$

B. *Results and investigations*

To investigate the proposed shields influence on the inductive power transmission system, a measurement of coil self-inductance (Fig.7 (a) and (b)), quality factor (Fig.8 (a) and (b)) for different ferrite powder concentrations and thicknesses (T1 and T2) in a frequency of 100 kHz was presented. Results shows that by increasing the ferrite concentrations presented in Table I, the measured coil-inductance increases from 17 µH in case of air-core coil to 19.5 µH for the sample 10 with a thickness T1 and a concentration of 85 wt.% of ferrite powder. In case of thickness T2 and under the same ferrite concentration the measured self-inductance was equal 20 µH. The equations of linearization of the measured self-inductances with different samples concentrations for the both thickness T1 and T2 are shown in Eq.20 and Eq.21, respectively. An error of self-inductance around ±2.5% and ±3% for the thicknesses T1 and T2 respectively. These errors can be due to many factors especially the non-linear increasing of the concentration and thicknesses of the investigated samples. Based on Eq.20 and Eq.21, increasing the coils thicknesses, the coil self-inductance decreases of about 0.1 µH.

$$L_{T1i} = 0.2\ S_i + 17 \tag{20}$$

$$L_{T2i} = 0.3\ S_i + 17 \tag{21}$$

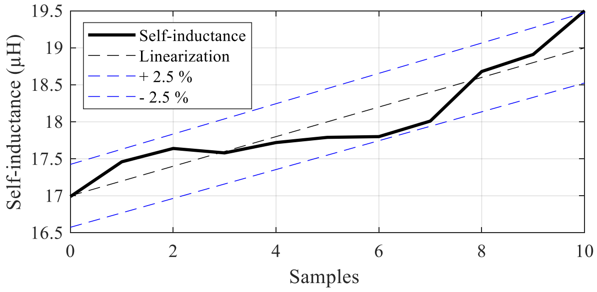

(a)

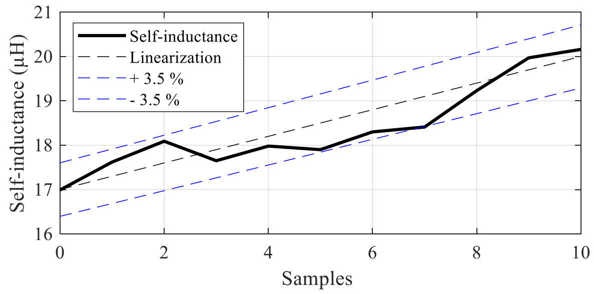

(b)

Fig. 7. Measured self-inductance for different samples concentration (a) Thickness T1 (b) Thickness T2

The measurement of the coils quality factors with T1 and T2 shields thicknesses has been presented in Fig.8 (a) and (b), respectively. Results shows that the increasing of the ferrite powder concentrations increases the system quality factor linearly with 6% as maximum of error for both samples thicknesses.

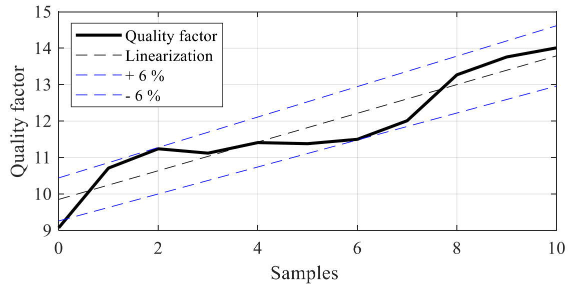

(a)

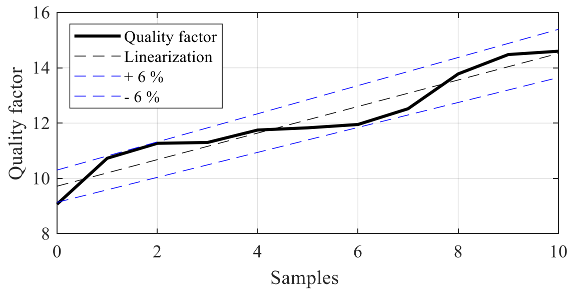

(b)

Fig. 8. Measured quality factor for different samples concentration (a) Thickness T1 (b) Thickness T2

Increasing the coil thickness increases the quality factor of about 0.1 as presented in linearity Eq.22 and Eq.23 for the thickness T1 and T2, respectively.

$$Q_{T1i} = 0.394\ S_i + 9.85 \tag{22}$$

$$Q_{T2i} = 0.48\ S_i + 9.72 \tag{23}$$

The error on the linearity can be due to the ferrite shields preparation, which present no linear steps of samples concentration and the error of the used samples thicknesses.

Fig.9 presents the measurement of the coupling factor of the prototypes with air-core coil and coils with associated ferrite powder thickness T2 and concentrations equal to 33.33 wt. %, 57.14 wt. % and 85 wt. %. The measured coupling factor increases almost linearly by increasing the ferrite powder concentrations.

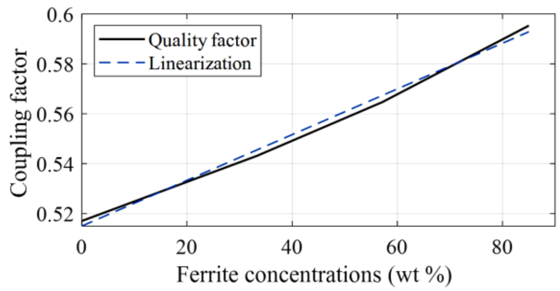

Fig. 9. Measured coupling factor of different concentrations

As presented in Eq.1, coil with high coupling factor and quality factor present the highest transmission efficiency. For that, a sending coil with a ferrite shield of 85 wt. % and thickness of 0.49 mm has been selected.

V. CONCLUSION

In this work, an investigation on flexible ferrite shields with different ferrite powder concentration and thicknesses is presented. A measurement of transmitter coil self-inductance and quality factor with different shields has been presented. Results shows that increasing the ferrite concentrations increases the self-inductance from 17.5 µH to 19.5 µH in the concentration 33 wt. % and 85 wt. %, respectively. With 85 wt. % of ferrite concentration, the self-inductances increase about 11.57 % and 15 % for thicknesses about 0.34 mm and 0.49 mm respectively. The IPT system efficiency depends especially on the coils quality factor and the coupling factor between transmitter and receiver coils. For that, a measurement of the coupling factor between air-core coil and shielded coil has been established. The increasing of the ferrite concentrations increases the coupling factor between the sending and the receiving coils from around 0.51 to 0.59.

Acknowledgment

The authors would like to thank the DAAD foundation for supporting their works within the project PRASEE.

References

[1] O. Kanoun et al., "Next Generation Wireless Energy Aware Sensors for Internet of Things: A Review," 2018 15th International Multi-Conference on Systems, Signals & Devices (SSD), Hammamet, 2018, pp. 1-6. 2018.

[2] M. P. Theodoridis, "Effective Capacitive Power Transfer," in *IEEE Transactions on Power Electronics*, vol. 27, no. 12, pp. 4906-4913, Dec. 2012.

[3] I. Chaour, A. Fakhfakh, O. Kanoun: "Enhanced passive RF-DC converter circuit efficiency for low RF energy harvesting". Sensors, 17, pp. 546. 2017.

[4] B. Kallel, O. Kanoun, H. Trabelsi: 'Large air gap misalignment tolerable multi-coil inductive power transfer for wireless sensors', IET Power Electronics, vol.9, no.8, pp.1768-1774, 2016.

[5] G. Bouattour, H. Ben Jemaa Derbel and O. Kanoun, "Multi-Parallel Sending Coils for Movable Receivers in Inductive Charging Systems," 2019 16th International Multi-Conference on Systems, Signals & Devices (SSD), Istanbul, Turkey, 2019, pp. 758-762.

[6] G. Guidi and J. A. Suul, "Minimizing Converter Requirements of Inductive Power Transfer Systems With Constant Voltage Load and Variable Coupling Conditions," in *IEEE Transactions on Industrial Electronics*, vol. 63, no. 11, pp. 6835-6844, Nov. 2016.

[7] A. Trigui, S. Hached, A. C. Ammari, Y. Savaria and M. Sawan, "Maximizing Data Transmission Rate for Implantable Devices Over a Single Inductive Link: Methodological Review," in *IEEE Reviews in Biomedical Engineering*, vol. 12, pp. 72-87, 2019.

[8] A. Ahmad, M. S. Alam and R. Chabaan, "A Comprehensive Review of Wireless Charging Technologies for Electric Vehicles," in *IEEE Transactions on Transportation Electrification*, vol. 4, no. 1, pp. 38-63, March 2018.

[9] E. Waffenschmidt, "Wireless power for mobile devices," *IEEE 33rd International Telecommunications Energy Conference (INTELEC)*, Amsterdam, 2011, pp. 1-9, 2011.

[10] J. Gao, "Inductive power transmission for untethered micro-robots," *31st Annual Conference of IEEE Industrial Electronics Society, 2005. IECON 2005.*, Raleigh, NC, 2005, pp. 6 pp.

[11] W. Chen, W. Lu, "Circuit modeling and efficiency analysis for wireless power transfer system with shielding, " International journal of circuit theory and applications, vol. 47, Issue 2, pp 294-303, December 2018.

[12] G. Bouattour, H. Ben Jemaa Derbel and O. Kanoun, "Multi-Parallel Sending Coils for Movable Receivers in Inductive Charging Systems," *2019 16th International Multi-Conference on Systems, Signals & Devices (SSD)*, Istanbul, Turkey, 2019, pp. 758-762, March 2019.

[13] M. Maass, A. Griessner, V. Steixner, C. Zierhofer, "Reduction of eddy current losses in inductive transmission systems with ferrite sheets, " BioMedical Engineering OnLine. Vol 16, January 2017.

[14] B. Park, J. Park, Y. Shin, Ch. Park, S. Ahn, Il S. Han, J. Jeong, K. S. Lee, "Wireless Charging System Using Soft Magnetic Composite for Unmanned Aerial Vehicle, " International journak of communications, vol 2, 2017.

[15] M. Bissannagari, T.H. Kim, J.G. Yook, J. Kim, "All inkjet-printed flexible wireless power transfer module: PI/Ag hybrid spiral coil built into 3D NiZn-ferrite trench structure with a resonance capacitor," Nano Energy, Vol 62, pp 645-652, August 2019.

[16] M. Young, The Technical Writer's Handbook. Mill Valley, CA: University Science, 1989.